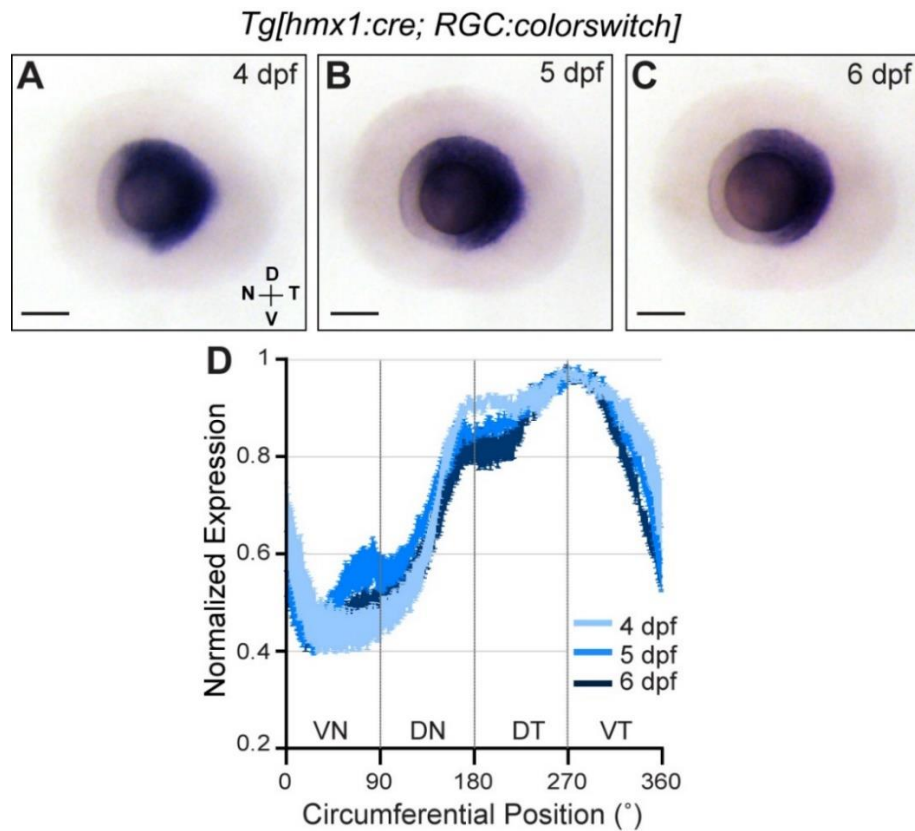
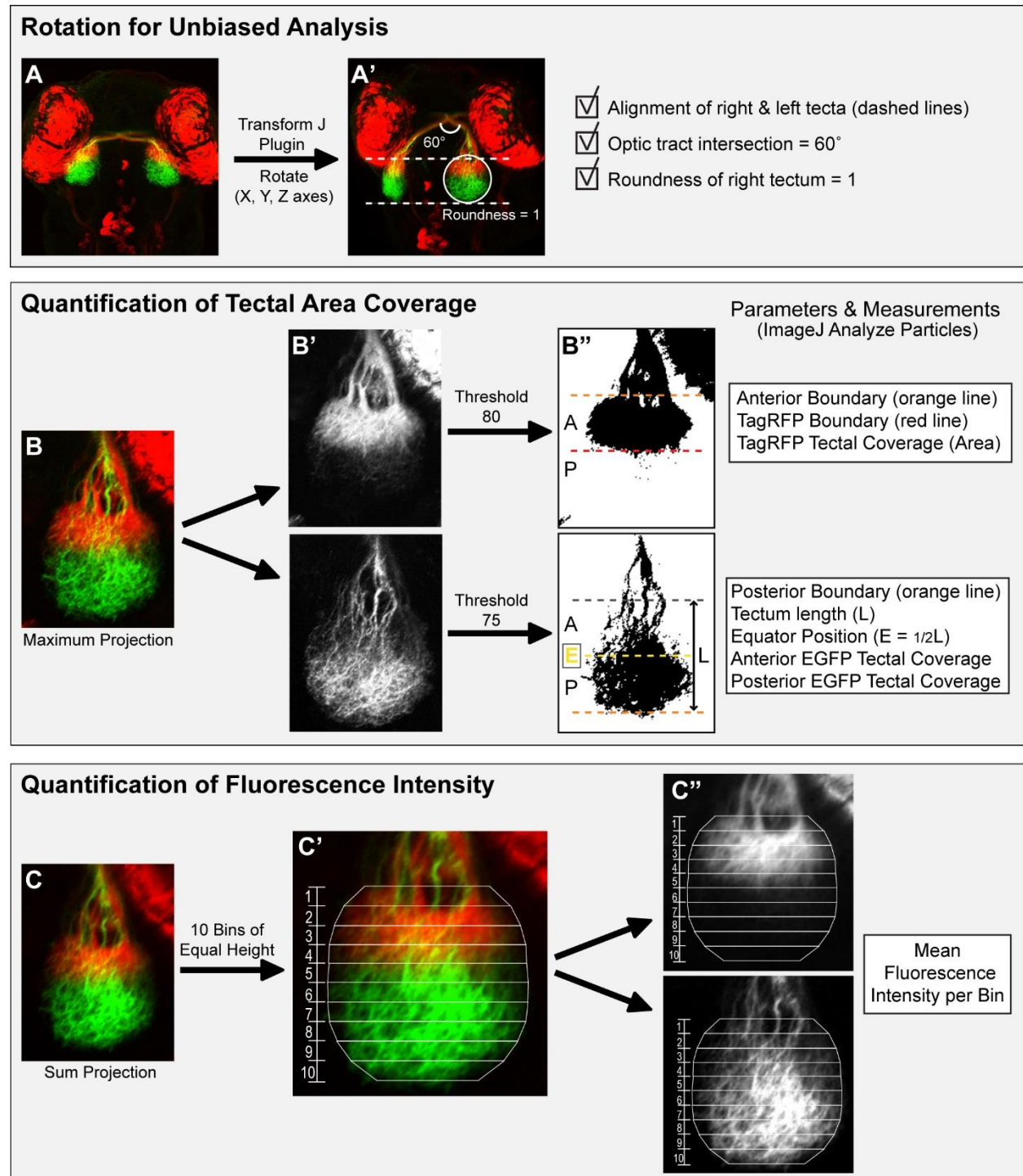


**Fig. S1. *Hmx4* is expressed in a nasal-high to temporal-low gradient in the retina.** Lateral (A-D) and dorsal (A'-D') views of whole embryos stained for *hmx4* by ISH. (A,A') At 24 hpf, *hmx4* is expressed in the developing lens (l) and is also weakly expressed in the retina (r) and otic vesicle (ov). (B,B') At 48 hpf, *hmx4* expression is strongly detected in the anterior retina, the otic vesicle and pharyngeal arches (pa). (C,C') *Hmx4* expression remains consistent at 72 hpf. (D,D') By 96 hpf, *hmx4* remains strongly expressed in the anterior retina and is still detected in the otic vesicle and pharyngeal arches, although to a lesser extent. (B''-D'') Lateral views of eyes dissected from embryos stained for *hmx4* by ISH. *Hmx4* has a high-nasal to low-temporal graded expression in the RGC layer of the retina at 48, 72 and 96 hpf. Scale bar: 200  $\mu$ m in A-D'; 50  $\mu$ m in E-F.

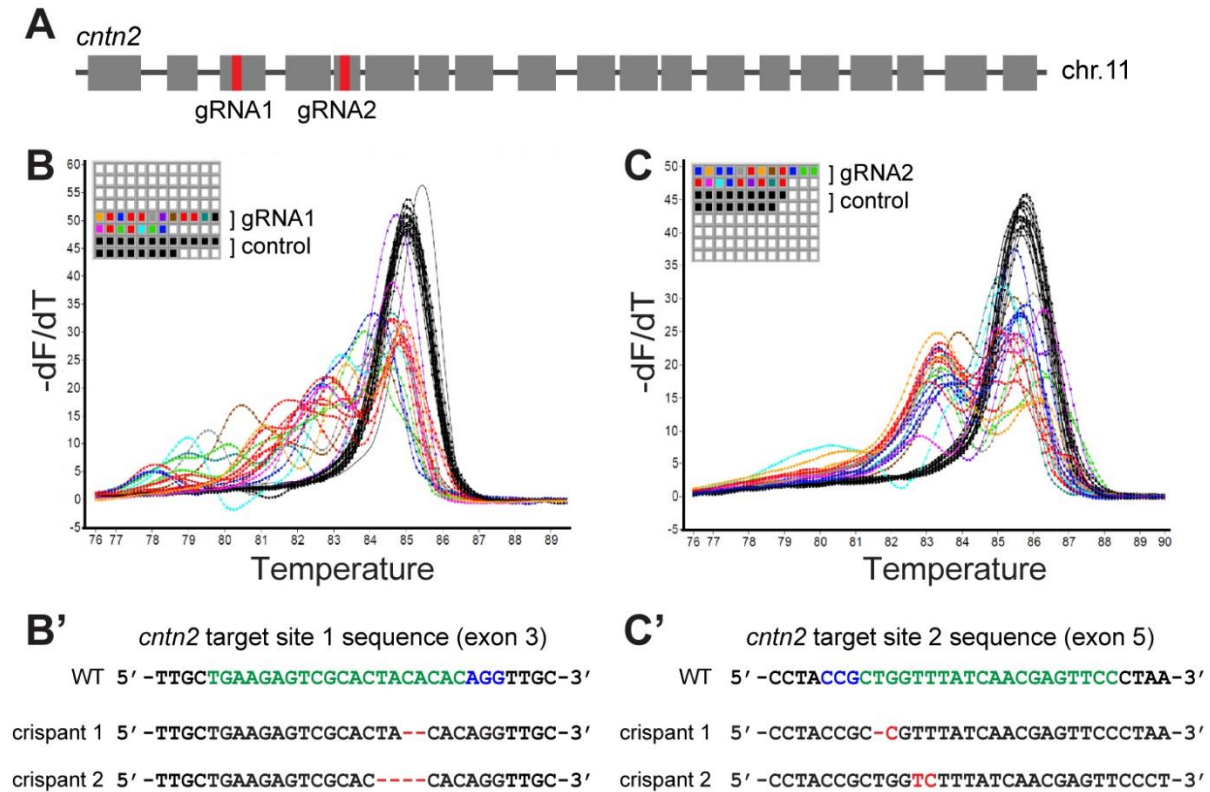


**Fig. S2. Cre-mediated recombination in the nasal retina occurs throughout retinal development.** (A-C) Lateral views of eyes dissected from [*hmx1-En2:cre* ; *RGC:colorswitch*] transgenic embryos and stained for *tagRFP* by ISH. *TagRFP* is only detected the temporal RGC layer and is not detected in nasal RGCs at 4, 5 and 6 dpf. Scale bars: 50  $\mu$ m. (D) Quantification of *tagRFP* retinal expression along a clockwise 360° trajectory shows that *tagRFP* expression is restricted to the temporal RGC layer.

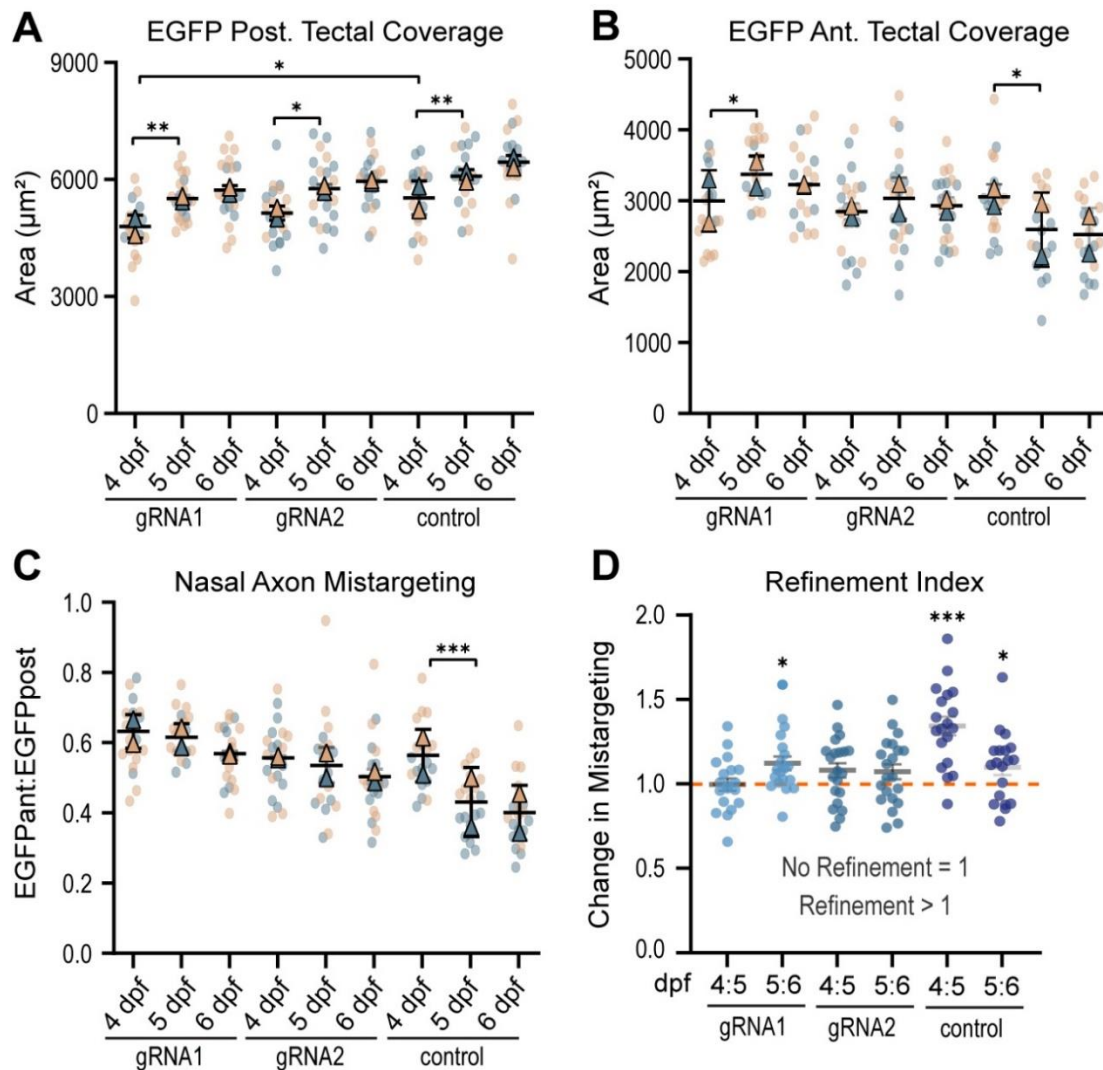


**Fig. S3. Visualization and quantification of A/P retinotopic mapping.** (A,A') Confocal stacks taken from a dorsal view were rotated along the X, Y, and Z-axes using the TransformJ plugin in ImageJ to obtain a consistent orientation between embryos. All stacks were rotated so that the left and right tecta were aligned horizontally, both optic tracts intersect at an angle of 60°, and the tectal roundness was equal to

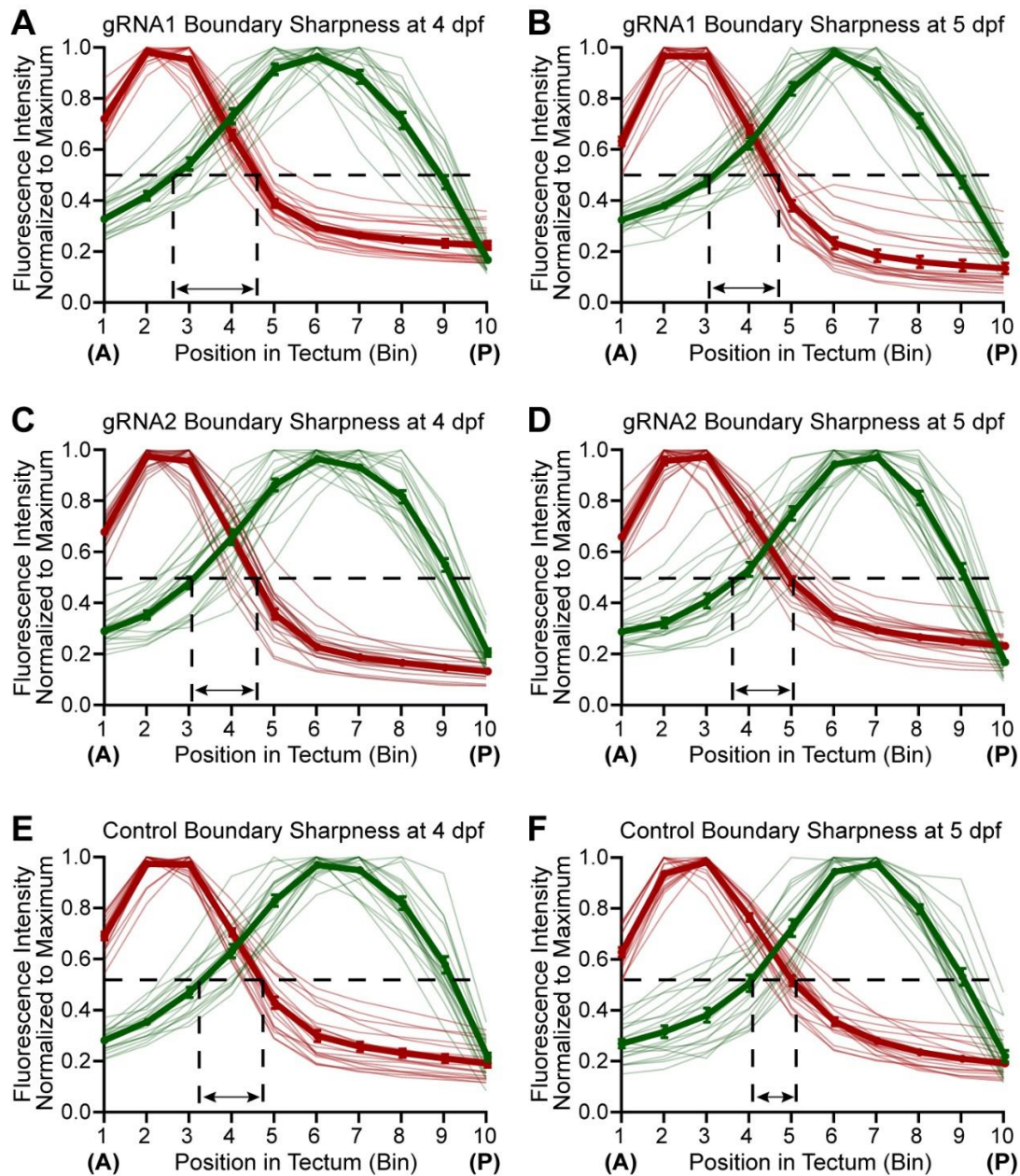
1. **(B-B'')** Quantification of tectal area coverage. **(B,B')** Rotated stacks were first maximum-projected. **(B'')** TagRFP and EGFP maximal projections were binarized with a threshold of 80 and 75, respectively. The binarized TagRFP maximal projection was used to delineate the anterior tectal boundary and the TagRFP boundary position. The tectal coverage area of TagRFP-positive temporal axons was measured using the Analyze Particles tool in ImageJ. The binarized EGFP maximal projection was used to delineate the posterior tectal boundary. The total tectum length (L) between the anterior and posterior tectal boundaries was measured, and the Equator (E) was set at  $\frac{1}{2}$  the total tectum length. The Analyze Particles tool was used to measure the tectal coverage area of the EGFP-positive nasal axons in the anterior (rostral to E) and posterior (caudal to E) halves of the tectum. **(C-C'')** Analysis of fluorescence intensity at the tectum. **(C)** Confocal stacks were sum-projected. **(C')** The tectum was divided into 10 bins of equal height using the polygon selection tool, with Bin1 being the anterior-most bin and Bin10 being the posterior-most bin. **(C'')** The mean fluorescence intensity of TagRFP and EGFP signals was measured within each bin using ImageJ.



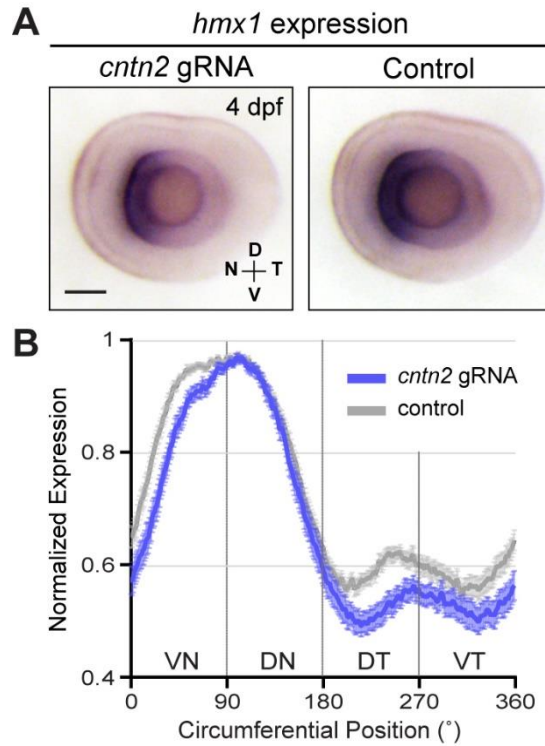
**Fig. S4. *Cntn2* RNP complexes induce mutations in G0 injected larvae.** (A) Schematic representation of the *cntn2* gene on chromosome 11 (chr11:23,933,017-23,988,258 in GRCz11). Two independent target sequences were chosen in exon 3 (gRNA1) and exon 5 (gRNA2) (red bars). (B,C) HRMA detection of *cntn2* mutations in individual larvae injected with *cntn2* gRNAs (*cntn2* crispants) or with Cas9 only (control, back curves). Mutations are detected in 18/19 (94.7%) gRNA1-injected larvae and in 21/21 (100%) gRNA2-injected larvae analyzed in this study. (B',C') Sequences of mutations in *cntn2* crispants. The sequence of each target site is indicated in green, with the PAM shown in blue. Examples of mutations detected in individual larvae are shown in red.



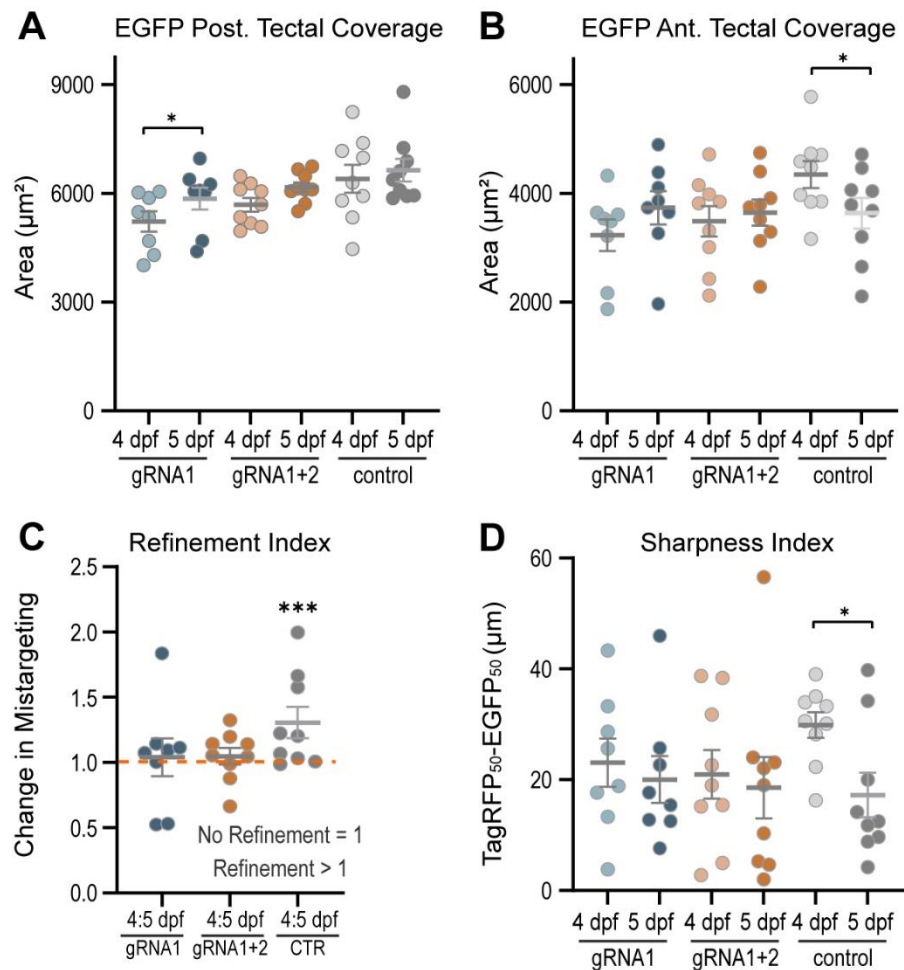
**Fig. S5. Nasal axon refinement defects persist at late stages in *cntn2* crispants.** (A) The area covered by nasal axons in the posterior half of the tectum significantly increases in *cntn2* crispants and controls. (B) The area covered by nasal axons in the anterior tectal half does not decrease between 5 and 6 dpf in crispants, indicating an absence of refinement at later stages in crispants. (C) The Nasal Axon Mistargeting Index remains unchanged at 6 dpf in crispants. (D) The refinement Index averages 1 in crispants from 4 to 6 dpf, confirming that the nasal projection domain does not refine at later stages in *cntn2* crispants. Means  $\pm$  SEM. n = 19 gRNA1 crispants, 21 gRNA2 crispants, 19 controls.



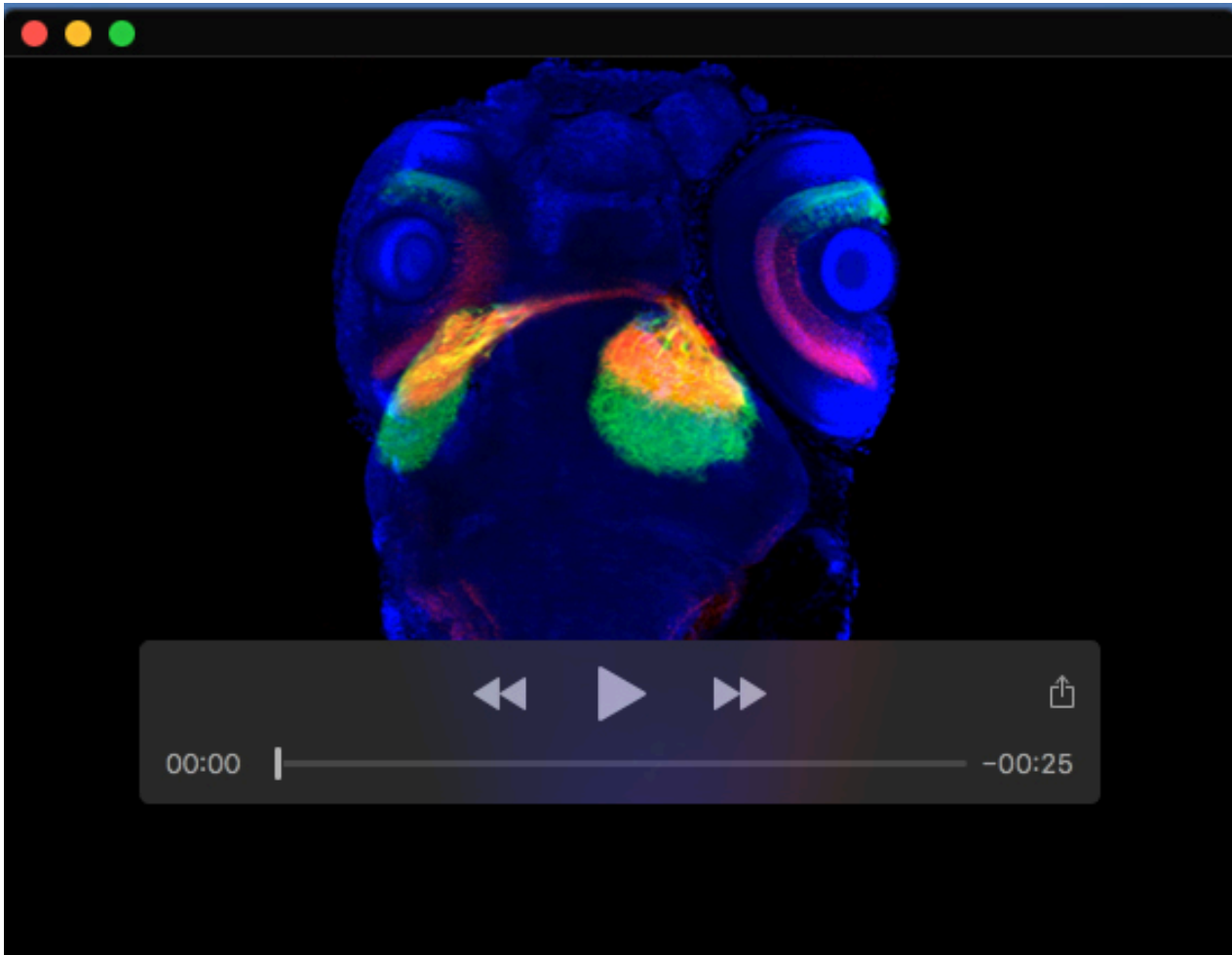
**Fig. S6. Cntn2 is necessary for the sharpening of the A/P retinotopic map.** Mean fluorescence intensities of EGFP and TagRFP were normalized to their respective maximum value and plotted along the A/P axis of the tectum. (A-D) The boundary sharpness between the temporal and nasal arborization domains (shown as the distance between EGFP<sub>50%</sub> and TagRFP<sub>50%</sub>) does not change significantly between 4 and 5 dpf in larvae injected with *cntn2* gRNA1 (A,B) or gRNA2 (C,D). (E,F) The boundary sharpness significantly decreases between 4 and 5 dpf in Cas9-injected control larvae, indicating the formation of a more precise antero-posterior retinotopic map. Data represent mean  $\pm$  SEM. *n* = 19 gRNA1-injected larvae, 21 gRNA2-injected larvae, 19 control larvae.



**Fig. S7. Retinal patterning is normal in *cntn2* crispants.** (A) Dissected eyes stained for *hmx1* by ISH. *Hmx1* is detected in the nasal RGC layer at 4 dpf in both *cntn2* crispants and Cas9-injected controls, indicating a normal retinal patterning in *cntn2* crispants. (B) Quantification of *hmx1* retinal expression. *Hmx1* expression is restricted to the nasal RGC layer in *cntn2* crispants.



**Fig. S8. *Cntn2* crisprants injecting with a cocktail of two *cntn2* gRNAs do not exhibit worse refinement and sharpening defects.** (A) The area covered by nasal axons in the posterior half of the tectum is comparable in *cntn2* crisprants and controls. (B) The area covered by nasal axons in the anterior tectal half does not decrease between 4 and 5 dpf in crisprants injected with gRNA1 or a combination of gRNA1 and gRNA2. (C) The refinement Index averages 1 in crisprants injected with gRNA1 or a combination of gRNA1 and gRNA2. (D) Instead of decreasing like in controls, the Sharpness Index remains stable and comparable in crisprants injected with gRNA1 or a combination of gRNA1 and gRNA2. Means  $\pm$  SEM.  $n = 8$  gRNA1 crisprants, 9 gRNA1 + gRNA2 crisprants, 9 controls.



**Movie 1.** 3D rendered movie of an [*hmx1-En2:cre; RGC:colorswitch*] double transgenic embryo immunostained for TagRFP and EGFP at 4 dpf. Confocal stacks taken from a dorsal view are rotated along the x-axis. To-Pro-3 was used as a nuclear counterstain to visualize the tectal neuropil.